JOURNAL OF MATERIALS SCIENCE 26 (1991) 4643–4647

Tensile properties of fine-grained 7475 aluminium alloy at various temperatures and strain rates

HIROHIKO TAKUDA*, SHIOMI KIKUCHI‡, NATSUO HATTA*
*Departments of *Mineral Science and Technology, and ‡Metal Science and Technology, Kyoto University, Sakyo-ku, Kyoto 606, Japan*

For a superplastic 7475 alloy, tensile properties are tested under various conditions in order to investigate the effects of the tensile conditions on the mechanical properties as well as on the microstructure after working. The results obtained here suggest a possibility of high-speed forming of this alloy. Under conditions of 400 °C and $8.3 \times 10^{-2}\,s^{-1}$ strain rate, a comparatively large elongation of about 200% can be attained. This may be due to the fact that the fine subgrains arise during the deformation. Also, mechanical properties at room temperature of the specimen prestrained under this condition are found to be fairly satisfactory.

1. Introduction

Since Wert and co-workers [1, 2] reported the thermo-mechanical process for making finer grain sizes of high-strength aluminium alloys, many studies [3–12] dealing with the superplasticity of 7475 alloy have been carried out from a mechanical as well as metallurgical point of view. However, there remain some practical problems in the superplastic forming of 7475 alloy, one of the most important being the improvement of forming speed.

The grain size of fine-grained 7475 alloy is commonly said to be 10 μm. Because of such a large grain size, the maximum elongation of 780% is obtained under conditions of strain rate = $2 \times 10^{-4}\,s^{-1}$ and temperature = 516 °C [9]. Such a low speed may be not advantageous to industrialization. However, the above maximum elongation is not practically required. Rather, an elongation of 200% or so may be regarded as satisfactory, if an increasing working speed can be attained.

In the present work, therefore, the fracture elongations of the 7475 alloy are investigated at various strain rates and temperatures. Secondly, the tensile properties of specimens at room temperature which have been stretched to a certain elongation under various conditions are examined. Furthermore, the results obtained are discussed in terms of the microstructural observations.

2. Experimental procedure

The test material was 7475 alloy sheet, of chemical composition as given in Table I. The tensile specimens were cut from a thin plate of 1.6 mm thickness in such a way as to be parallel to the rolling direction. Also, the gauge length was set to be 10 mm, as shown in Fig. 1.

The tensile tests were carried out in an infrared image furnace fitted to an Instron-type machine. The specimens were inserted into the furnace at room temperature and the tests were started after a waiting time of 30–60 min for the test temperatures of 300, 350, 400, 450 and 500 °C to be reached. During the tests the temperatures of the specimens were controlled to within ± 2 °C. The specimens were elongated to fracture by a constant crosshead velocity between 0.05 and 50 mm min^{-1}. The initial strain rates of the tensile tests ranged between 8.3×10^{-5} and $8.3 \times 10^{-2}\,s^{-1}$.

In addition to the normal tensile tests, the following tests were carried out. The specimens were deformed to an elongation of 100% under the above conditions, cooled rapidly, and then elongated to fracture at room temperature. The microstructural changes in the specimens were observed at an elongation of 100%, by both optical and transmission electron microscopy.

3. Results and discussion

3.1. Normal tensile tests

Fig. 2 shows the relation between the fracture elongation and the temperature for various initial strain rates. The maximum elongation of 730% is obtained under conditions of 500 °C and $8.3 \times 10^{-5}\,s^{-1}$. These may be similar conditions to those reported in the literatures [2, 9], i.e. 516 °C and $2 \times 10^{-4}\,s^{-1}$. When the initial strain rate is $8.3 \times 10^{-5}\,s^{-1}$, the elongation drops rapidly and monotonically with decreasing temperature. When the initial strain rate is set at $8.3 \times 10^{-4}\,s^{-1}$, the elongation reaches a maximum value at 500 °C (≃ 400%) and drops monotonically with decreasing temperature. However, in cases where the initial strain rate is 8.3×10^{-3} and $8.3 \times 10^{-2}\,s^{-1}$, the peak values of elongation appear around 400 °C.

0022–2461/91 $03.00 + .12

TABLE I Chemical composition of the 7475 alloy (wt %)

Si	Fe	Cu	Mn	Mg	Cr	Zn	Ti	Al
0.04	0.08	1.52	tr.	2.61	0.21	5.74	0.02	bal.

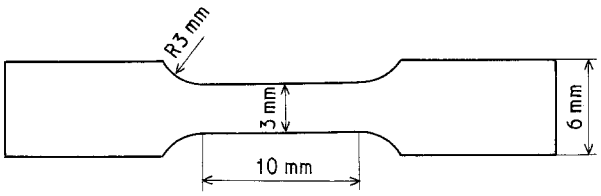

Figure 1 Tensile specimen.

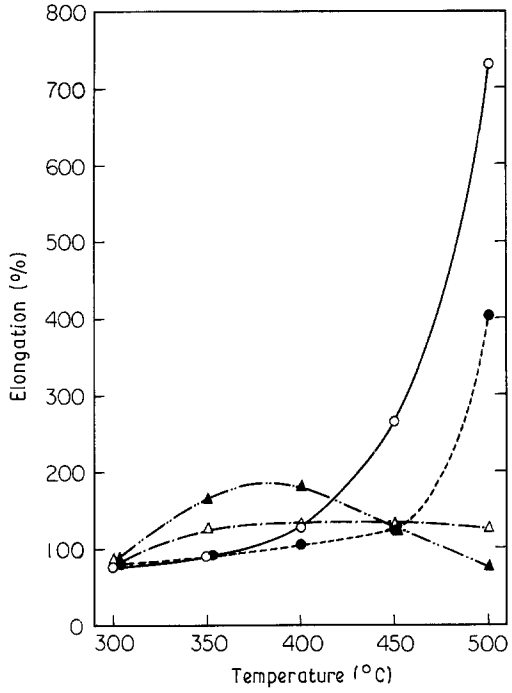

Figure 2 Relationship between temperature and fracture elongation for various initial strain rates: (○) $8.3 \times 10^{-5}\,s^{-1}$; (●) $8.3 \times 10^{-4}\,s^{-1}$; (△) $8.3 \times 10^{-3}\,s^{-1}$, (▲) $8.3 \times 10^{-2}\,s^{-1}$.

Here, it is remarkable that a fairly large elongation of about 200% is obtained at 400 °C and $8.3 \times 10^{-2}\,s^{-1}$.

Fig. 3 shows the relation between the fracture elongation and the initial strain rate for three different temperatures. In the figure the strain rate is indicated on a logarithmic scale. At 500 °C the elongation decreases with increasing strain rate, and falls at 100% near the strain rate of $10^{-2}\,s^{-1}$. On the other hand, the elongation at 400 °C has a tendency to increase with strain rate. At the lower temperature of 300 °C the elongation remains almost unvaried below 100%.

The experimental data concerning strain-rate sensitivity for superplastic deformation have been described previously [2, 9], therefore, the strain sensitivity, i.e. work hardening, only is discussed further here. From the stress–strain relation the work-hardening exponent, n, may be expressed in the form

$$\sigma = a\varepsilon^n \qquad (1)$$

where σ is the stress, a a constant, and ε log strain. Fig. 4a shows the relation between the work-hardening exponent from 0.1–0.4 strain (from about 10%–50% elongation) and the initial strain rate for various temperatures. Here, n values from 0.1–0.4 strain are calculated by

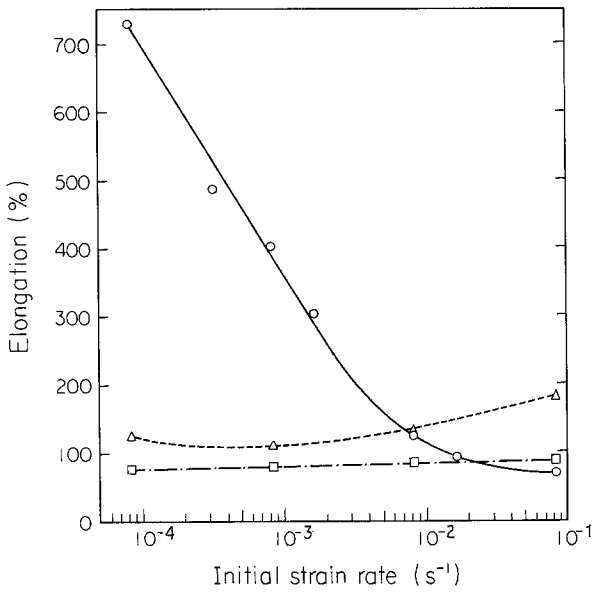

Figure 3 Relationship between initial strain rate and fracture elongation at (□) 300, (△) 400 and (○) 500 °C.

$$n = \frac{\log \sigma_{(\varepsilon = 0.4)} - \log \sigma_{(\varepsilon = 0.1)}}{\log 0.4 - \log 0.1} \qquad (2)$$

In the figure, n values below zero indicate work softening or the occurrence of necking. At the lower strain rates and higher temperatures there is a group whose n values are positively large. This group corresponds to the very large elongations seen in Figs 2 and 3. This kind of work hardening is considered to be based on the grain growth during deformation [13]. With increase in the strain rate, n decreases once below zero and recovers to zero or slightly positive values, for all temperatures.

Next, the work hardening exponents from 0.1–0.7 strain (from about 10%–100% elongation) are shown in Fig. 4b. The n values are still positive for the cases where the large elongations are observed. With increase in strain rate, n values at 500 °C fall noticeably. On the contrary, n values at 400 °C increase with strain rate and are slightly positive at $8.3 \times 10^{-2}\,s^{-1}$, corresponding to the fracture elongation of nearly 200% (see Figs 2 and 3). It may be judged from this n value that the negative phenomenon, such as necking or cavitation, does not occur to any great extent at an elongation of 100% under these conditions.

3.2. Tensile tests at room temperature after working

There were a number of cases in the tensile tests where elongations over 100% were obtained. In order to examine the influence of the tensile conditions on the mechanical properties after working, the specimens elongated by 100% under various conditions were again tested at room temperature.

Fig. 5a shows the relation between the fracture elongation at room temperature after working and the

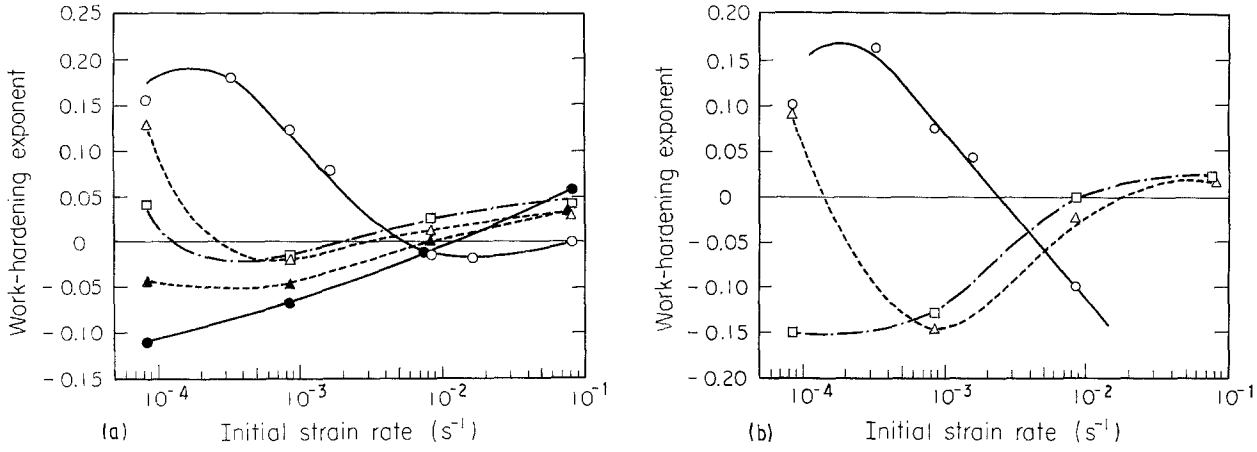

Figure 4 Relationship between initial strain rate and work-hardening exponent (a) from 0.1–0.4 strain, (b) from 0.1–0.7 strain. (○) 500 °C, (△) 450 °C, (□) 400 °C, (▲) 350 °C, (●) 300 °C.

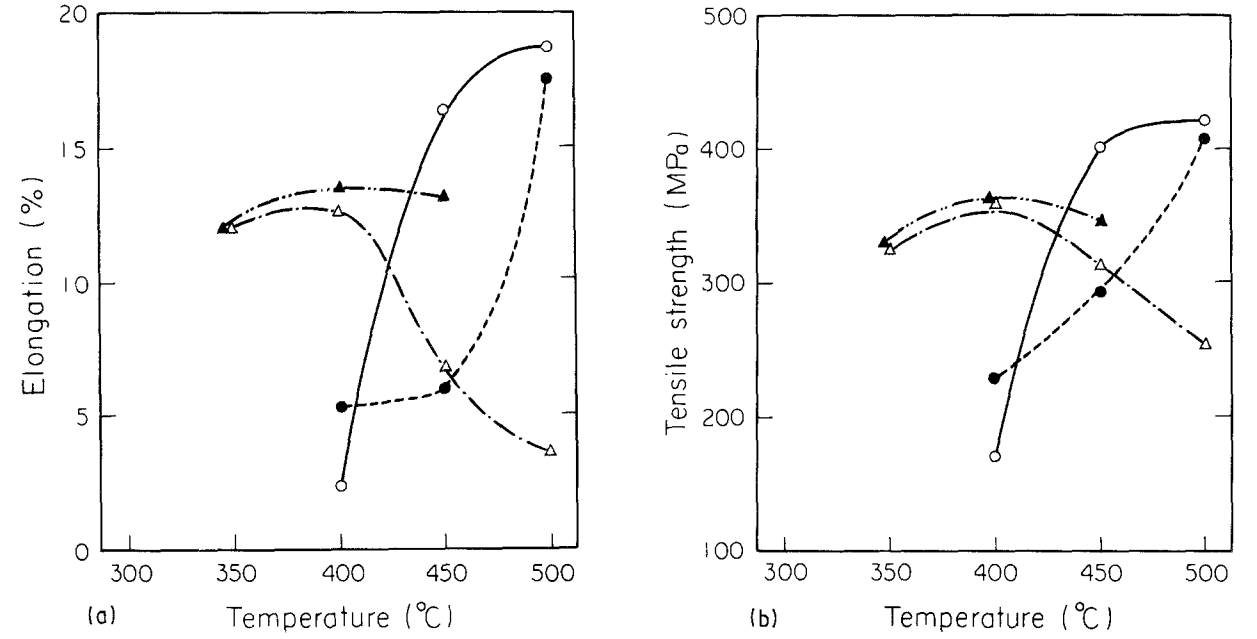

Figure 5 Effects of working conditions on mechanical properties at room temperature after working: (a) fracture elongation, (b) tensile strength. Initial strain rates: (○) $8.3 \times 10^{-5}\ s^{-1}$; (●) $8.3 \times 10^{-4}\ s^{-1}$; (△) $8.3 \times 10^{-3}\ s^{-1}$; (▲) $8.3 \times 10^{-2}\ s^{-1}$.

working temperature with initial working strain rate as a parameter. The specimens which were stretched under conditions of 500 °C and 8.3×10^{-5} and $8.3 \times 10^{-4}\ s^{-1}$ strain rate, exhibit comparatively large elongations. Again, conditions of 450 °C and $8.3 \times 10^{-5}\ s^{-1}$ give a large elongation above 15%. Although a little inferior to this group, another group exhibiting large elongation exists at a working temperature of approximately 400 °C and at a higher initial strain rate. The same tendency is recognized in Fig. 5b, which shows the variation of tensile strength at room temperature with working temperature. It can be understood from Figs 2, 5a and b that the specimens which were stretched under conditions where a large elongation can be obtained in the normal tensile tests, exhibit a larger tensile strength at room temperature.

3.3. Microstructural observations

Fig. 6 shows the microstructure of the specimen before tensile testing. The grain size ranges from 10–15 μm.

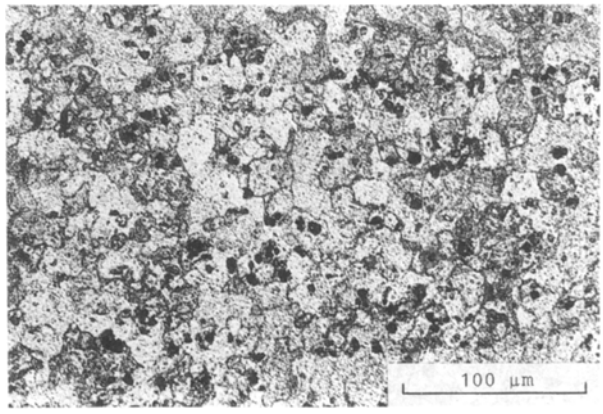

Figure 6 Microstructure of specimen before tensile testing.

Besides very fine precipitates of 0.05–0.1 μm (seen by TEM), many coarse precipitates can be seen with sizes of micrometre order.

Fig. 7a–d are optical micrographs of the specimens after an elongation of 100% under various tensile

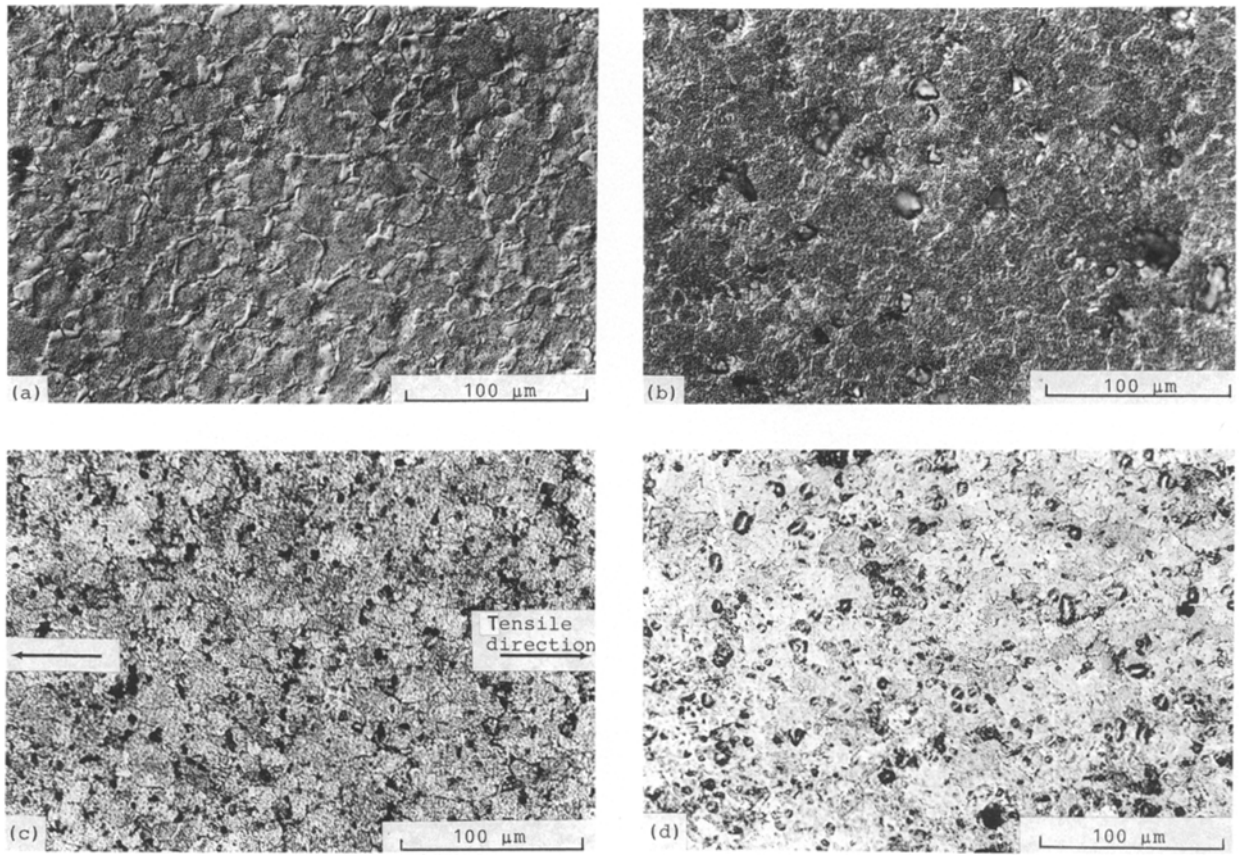

Figure 7 Microstructures of specimens after an elongation of 100% deformed under various temperatures and initial strain rates: (a) 500 °C, $8.3 \times 10^{-5}\ s^{-1}$; (b) 500 °C, $8.3 \times 10^{-3}\ s^{-1}$; (c) 400 °C, $8.3 \times 10^{-5}\ s^{-1}$; (d) 400 °C, $8.3 \times 10^{-2}\ s^{-1}$.

conditions. Fig. 7a shows the microstructure of the specimen elongated at 500 °C at an initial strain rate of $8.3 \times 10^{-5}\ s^{-1}$. It can be seen that the coarse precipitates annihilate and the grains grow somewhat, but remain equiaxed. This suggests that grain-boundary sliding governs the deformation.

Two typical microstructures of specimens elongated under conditions differing from the optimal are shown in Fig. 7b and c: one is the case of higher strain rate at 500 °C (b), and the other the case of lower temperature at $8.3 \times 10^{-5}\ s^{-1}$ strain rate (c). The grains in Fig. 7b are equiaxed similar to the grain morphology in Fig. 7a, but a fairly large number of cavities is observed in Fig. 7b. On the other hand, it can be seen in Fig. 7c that the coarse precipitates do not annihilate and each grain is stretched in the tensile direction. This indicates that the grains deform themselves. As was found in Fig. 5a, the fracture elongations of the specimens pre-deformed under the conditions of Fig. 7b and c are small. It is considered that these small ductilities result from such microstructural disadvantages, i.e. cavities (b) and elongated grains (c).

Fig. 7d shows the microstructure obtained at 400 °C and an initial strain rate of $8.3 \times 10^{-2}\ s^{-1}$. This microstructure seems entirely different from the others. As ascertained from the transmission electron micrograph (Fig. 8), there are many fine subgrains. The 7475 alloy is a precipitate hardening alloy and at the same time a solid solution hardening alloy. During deformation of the solid solution hardening alloys at high temperature the dislocation motion tends to be viscous, and generally the dislocation arrangement is uniform [14]. However, when the strain rate becomes higher, the viscous motion of dislocations with the Cottrell atmosphere is broken. In this case, the dislocations pile up and cause subgrains to form [15]. The occurrence of the fine subgrains in the present experiment is considered to be based on such a phenomenon, and leads to the comparatively large elongation (see Figs 2, 3 and 5a).

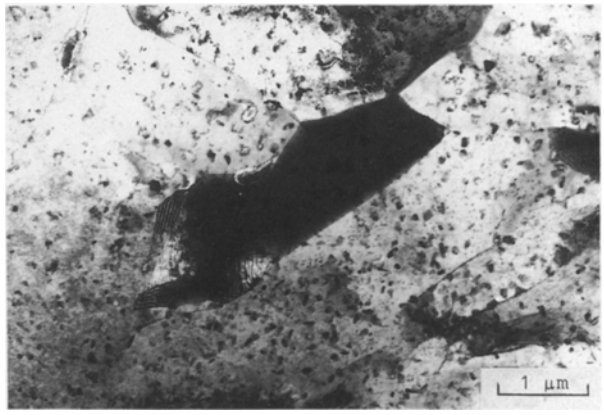

Figure 8 Transmission electron micrograph of specimen after an elongation of 100% deformed at 400 °C and $8.3 \times 10^{-2}\ s^{-1}$ initial strain rate.

4. Conclusion

In order to examine the possibility of high-speed deformation of superplastic 7475 alloy, tensile tests

were carried out under various strain rates and temperatures. The tensile properties at room temperature and the microstructures of the specimens pre-strained under various strain rates and temperatures were also investigated.

It was found that a comparatively large elongation may be attained at a high strain rate of the order of $10^{-2}\,s^{-1}$. In the present experiments, an elongation of nearly 200% was obtained at 400 °C and $8.3 \times 10^{-2}\,s^{-1}$ initial strain rate. The tensile properties at room temperature of the specimen deformed under these conditions are also comparatively satisfactory. The microstructural characteristics obtained with these conditions are fine subgrains which arise during deformation. If the occurrence of these fine subgrains can be positively controlled, the possibility of high-speed deformation of 7475 alloy might be expected.

Acknowledgements

The authors thank Sky Aluminium Co. Ltd for supplying fine-grained 7475-Al sheets. H. Takuda thanks the Japanese Ministry of Education with Grant-in-Aid for Encouragement of Young Scientists for financial support.

References

1. J. A. WERT, N. E. PATON, C. H. HAMILTON and M. W. MAHONEY, *Met. Trans.* **12A** (1981) 1267.
2. N. E. PATON, C. H. HAMILTON, J. WERT and M. MAHONEY, *J. Metals* **34** (1982) 21.
3. C. C. BAMPTON and J. W. EDINGTON, *Met. Trans.* **13A** (1982) 1721.
4. *Idem., Trans. ASME. J. Engng Mater. Technol.* **105** (1983) 55.
5. M. W. MAHONEY, C. H. HAMILTON and A. K. GHOSH, *Met. Trans.* **14A** (1983) 1593.
6. J. PILLING and N. RIDLEY, *Acta Metall.* **34** (1986) 669.
7. Y. KOBAYASHI, H. GOTO and Y. TAKEUCHI, *J. Jpn Inst. Light Metals* **36** (1986) 36.
8. A. JUHÁSZ, N. Q. CHINH, P. TASNÁDI, I. KOVÁCS and T. TURMEZEY, *J. Mater. Sci.* **22** (1987) 137.
9. Y. HIROSE, Y. MIYAGI, M. HINO and T. ETO, *Aluminium* **63** (1987) 386.
10. Ph. BOMPARD, J. Y. LACROIX and A. VARLOTEAUX, *ibid.* **64** (1988) 162.
11. K. MATSUKI, G. STANIEK, H. NAKAGAWA and M. TOKIZAWA, *Z. Metallkde* **79** (1988) 231.
12. Y. HONG, N. MURAMATSU and T. ENDO, *J. Jpn Inst. Light Metals* **39** (1989) 541.
13. C. H. CÁCERES and D. S. WILKINSON, *Acta Metall.* **32** (1984) 415.
14. R. HORIUCHI and M. OTSUKA, *Trans. Jpn Inst. Metals* **13** (1972) 284.
15. P. YAVARI and T. G. LANGDON, *Acta Metall.* **30** (1982) 2181.

Received 27 November 1989
and accepted 18 July 1990